Jagannath University Journal of Science
Volume 07, Number I, December 2020, pp. 1-8
https://jnu.ac.bd/journal/portal/archives/science.jsp
ISSN 2224-1698

JnUJSci

Mixed Convective Non-Newtonian Flow along an Isothermal Sphere

Research Article

Md. Mafujul Haque[1], Sidhartha Bhowmick[1*], Md. Mamun Molla[2]

[1]*Department of Mathematics, Jagannath University, Dhaka, Bangladesh*
[2]*Department of Mathematics & Physics, North South University, Bangladesh*

Received: 01 October 2020
Accepted: 29 November 2020

Abstract : Two dimensional mixed convective boundary-layer flow of non-Newtonian fluids over an isothermal sphere has been considered by modified power-law viscosity technique. No infinite viscosity arises in this technique; therefore, removable singularities are presented in the formulation of boundary-layer. Thus, applying the implicit finite difference method with marching order by double sweep method the boundary-layer equations can solve numerically. These simulations are revealed for the shear thinning and shear thickening fluids due to the velocity and temperature distributions of the fluid. Moreover, shearing stress and heat transfer rate are also calculated and discussed in accordance with the local skin-friction coefficient and local Nusselt number.

Keywords: *Mixed convection ● Non-Newtonian fluid ● Isothermal sphere*

1. Introduction

The mixed convective boundary-layer flow of 2-dimensional non-Newtonian fluid over an isotherm sphere represents an important part in many manufacturing cases which are associated with pseudoplastic fluids. At very low shear rates, these fluids behaves like constant viscosity. Again a viscosity is constant once the shear rate is high and is decreases continuously with intermediate shear rate. Apparent viscosity will commence to decrease if the shear rate is increased beyond a particular value. The fluid becomes Newtonian once the share rate is high with a uniform visible viscosity.

Several analytical and experimental research works in Newtonian fluids have been done to heat transfer from a sphere, but mixed convective non-Newtonian fluids over a sphere has received less attention till now. Chiang *et al*. (1964) examined the natural convection along a sphere by given surface temperature as well as heat flux. Free convection along a sphere with puffing and absorption was investigated by Huang *et al*. (1987). Chen and Mucoglu (1977) has been performed the analyses of all the convections regarding a spherical geometry. Nazar *et al.* (2002) studied the natural convective flow over a sphere with uniform surface temperature in micro-polar fluid. As far as the authors know, mixed convective non-Newtonian fluid over an isotherm sphere has not been investigated yet. Thus the current work is used to fill vacancies.

Boger (1977) delivered an excellent experimental investigation about non-Newtonian fluid. He exhibited a data set for the pseudo plastic fluid. Firstly an analytical study for such fluid is studied by Acrivos (1960), which contains the nonrealistic physical limit of zero and nonfinite viscosity showed by conventional power-law method. Thereafter, a wide range of papers have been reveled in non-Newtonian fluids like polymers, chemicals, melted plastics, foods and petroleum and mineral production and various natural phenomena, which were impracticable.

*Corresponding Author: Sidhartha Bhowmick
E-mail: *sidharthabhowmick@yahoo.com*

Nazar *et al.* (2002; 2003) investigated the mixed convective boundary-layer flow around a solid sphere with constant cases in viscous as well as micro polar fluids, respectively. Salleh *et al.* (2010) revealed on Newtonian heating. Yacob and Nazar (2006) studied on constant heat flux case and then Kotouc *et al.* (2008) who investigated the losing of axisymmetry through a warmed sphere for the mixed convection case. Huang *et al.* (1989) considered the natural convective flow with the effects of Prandtl number by implicit finite difference technique. E. Kim (1997) used the finite volume technique to study the free convective flow with a vertical wavy surface, which presents the impractical outcomes at the top edge. The analyses of Chen and Mucoglu (1978), those have been studied on mixed convective flow over an isotherm heat flux sphere, rely on the normalized mixed convective parameter $\lambda = Gr / Re^2$, where *Re* and *Gr* are Reynolds number and Grashof number, respectively.

The proposed revised power-law technique is sketched in Fig. 1 with the power index n = 0.6, 0.8, 1.0 1.2, 1.4; where n = 1.0 is for Newtonian fluids and the method is expressed by investigational data of the non-Newtonian fluids (Boger, 1977). No infinite viscosity arises in this and removable singularities represented in the formulation of boundary-layer. The model, actually, fits measured viscosity data well. The given values in the technique may fix with existing quantities that are defined in details in Yao and Molla (2008). For shear-thinning fluid the outcomes for mixed convective non-Newtonian flow over a vertical surface by the revised power-law technique was showed by Molla and Yao (2009).

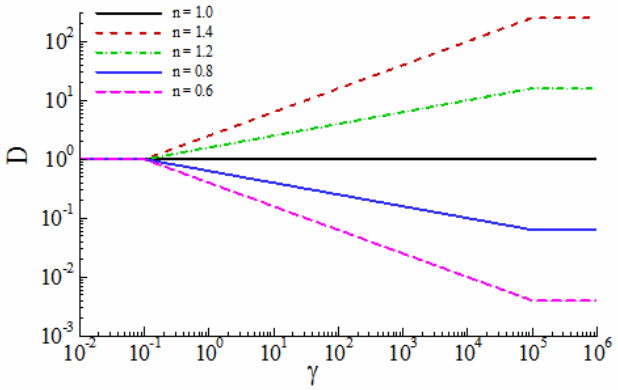

Figure 1: Revised power-law relations for n = 0.6, 0.8, 1.0, 1.2, 1.4 while $\gamma_1 = 0.1, \gamma_2 = 10^5$.

For the instance of pseudoplastic fluids the boundary-layer formulation on natural convection with an isotherm and heat-flux horizontal cylinder are numerically revealed in Bhowmick *et al.* (2013a; 2013b). Bhowmick *et al.* (2014a; 2014b) also investigated the mixed convective flow over an isotherm horizontal cylinder as well uniform heat-flux case by this modified power-law model. Those give the reasonable results of the boundary-layer including the both edges.

In this investigation, the behavior of non-Newtonian fluids on the mixed convective flow along a sphere with uniform temperature are considered by taking the power-law index n to completely reveal the development of the non-Newtonian fluids.

2. Problem formulations

Two dimensional laminar mixed convective boundary-layer steady non-Newtonian flow along an isothermal sphere with radius 'a' with a buoyancy force $g\beta(T - T_\infty)\sin(\bar{x}/a)$ has been considered. We also consider the instantaneous development of inviscid flow along the spherical surface with the velocity, $\bar{u}_e(\bar{x}) = \mathrm{U}_\infty \sin(\bar{x}/a)$, here U_∞ is considered freestream velocity.

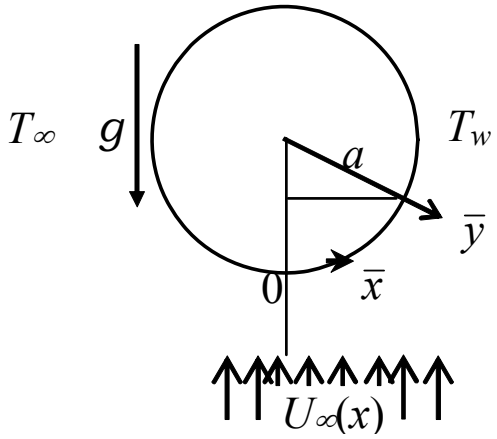

Figure 2: Flow model with coordinating system

The shear rate is depended on the viscosity and related by a model, which name is modified power-law viscosity model. For the case of non-Newtonian fluids we may describe the shear-thickening as well as the shear-thinning fluids. Here we may assume that $T_w > T_\infty$, where T_w is the surface temperature and T_∞ is the ambient temperature (see Fig. 2).

From the above discussions, the governing flow and heat transfer equations are:

$$\frac{\partial(\bar{r}\,\bar{u})}{\partial\bar{x}} + \frac{\partial(\bar{r}\,\bar{v})}{\partial\bar{y}} = 0 \qquad (1)$$

$$\rho\left(\bar{u}\frac{\partial\bar{u}}{\partial\bar{x}}+\bar{v}\frac{\partial\bar{u}}{\partial\bar{y}}\right)=\rho\bar{u}_e\frac{d\bar{u}_e}{d\bar{x}}+\frac{\partial}{\partial\bar{y}}\left(\mu\frac{\partial\bar{u}}{\partial\bar{y}}\right)+\rho g\beta\left(T-T_\infty\right)\sin\left(\frac{\bar{x}}{a}\right) \quad (2)$$

$$\bar{u}\frac{\partial T}{\partial\bar{x}}+\bar{v}\frac{\partial T}{\partial\bar{y}}=\frac{k}{\rho C_p}\frac{\partial^2 T}{\partial\bar{y}^2} \quad (3)$$

Here the velocity components along the axes are $\bar{u}$ and $\bar{v}$, k is the thermal conductivity,$\rho$is the fluid density,$\mu$is the fluid viscosity, g is the gravitational force, C_p is the specific heat at constant pressure,β is the thermal expansion coefficient and T is the temperature of fluid.Modified power-law model is defined as follows by correlating with the kinematic viscosity ν (= μ/ρ) (see Bhowmick *et al.* 2014a in details).

$$\nu=\frac{K}{\rho}\left|\frac{\partial\bar{u}}{\partial\bar{y}}\right|^{n-1} \text{ for } \bar{\gamma}_1\le\left|\frac{\partial\bar{u}}{\partial\bar{y}}\right|\le\bar{\gamma}_2 \quad (4)$$

The present problems of the boundary conditions are:

$$\bar{u}=0,\quad \bar{v}=0,\quad T=T_w \qquad at \quad \bar{y}=0 \quad (5a)$$

$$\bar{u}\to\bar{u}_e(\bar{x}),\qquad T\to T_\infty \quad as \quad \bar{y}\to\infty \quad (5b)$$

The normalized variables are:

$$x=\frac{\bar{x}}{a},y=\frac{\bar{y}}{a}\mathrm{Re}^{1/2},u=\frac{\bar{u}}{U_\infty},v=\frac{\bar{v}}{U_\infty}\mathrm{Re}^{1/2},$$
$$\theta=\frac{(T-T_\infty)}{(T_w-T_\infty)},\ Gr=\frac{g\beta(T_w-T_\infty)a^3}{\nu_1^2},\ \nu_1=\frac{\mu_1}{\rho},$$
$$D=\frac{\nu}{\nu_1},\mathrm{Pr}=\frac{\nu_1\rho C_p}{k}, \quad (6)$$
$$u_e=\frac{\bar{u}_e}{U_\infty},\mathrm{Re}=\frac{U_\infty a}{\nu_1},\lambda=\frac{G_r}{\mathrm{Re}^2}.$$

Where, ν_1 is the reference viscosity, θ is the function of normalized fluid temperature, *Gr*, Re and Pr are the Grashof number, the Reynolds number and the Prandtl number, respectively. Replacing (6) into equations (1-4) we have,

$$\frac{\partial(ru)}{\partial x}+\frac{\partial(rv)}{\partial y}=0 \quad (7)$$

$$u\frac{\partial u}{\partial x}+v\frac{\partial u}{\partial y}=u_e\frac{du_e}{dx}+\frac{\partial}{\partial y}\left(D\frac{\partial x}{\partial y}\right)+\lambda\theta\sin x \quad (8)$$

$$u\frac{\partial\theta}{\partial x}+v\frac{\partial\theta}{\partial y}=\frac{1}{\mathrm{Pr}}\frac{\partial^2\theta}{\partial y^2} \quad (9)$$

$$D=\frac{\nu}{\nu_1}=\frac{K}{\rho\nu_1}\left|\frac{\partial\bar{u}}{\partial\bar{y}}\right|^{n-1}=\frac{K}{\rho\nu_1}\left|\left(\frac{U_\infty}{a\,\mathrm{Re}^{-1/2}}\right)\frac{\partial u}{\partial y}\right|^{n-1}$$
$$=\frac{K}{\rho\nu_1}\left(\frac{U_\infty}{a\,\mathrm{Re}^{-1/2}}\right)^{n-1}\left|\frac{\partial u}{\partial y}\right|^{n-1}=C\left|\frac{\partial u}{\partial y}\right|^{n-1} \quad (10)$$

Associated with the power-law we get the length scale:

$$a=\left[\frac{\kappa\,\mathrm{Re}^{3(n-1)/2}}{C\rho\nu_1}\right]^{1/2(n-1)} \quad (11)$$

The boundary conditions are:

$$u=0,\quad v=0,\quad \theta=1 \qquad \text{at} \quad y=0 \quad (12a)$$

$$u_e\to\sin x,\qquad \theta\to0 \quad \text{as} \quad y\to\infty \quad (12b)$$

Now we have to propose the parabolic transformations [Bhowmick *et al.*2013, 2014]:

$$X=x,\ Y=y,\ U=\frac{u}{x},\ V=v,\ \theta=\theta \quad (13)$$

Replacing the variables (13) in the equations (7-10) and simplify, we are getting the following transformed equation forms:

$$XU\cot X+X\frac{\partial U}{\partial X}+U+\frac{\partial V}{\partial Y}=0 \quad (14)$$

$$UX\frac{\partial U}{\partial X}+U^2+V\frac{\partial U}{\partial Y}=\frac{\sin X\cos X}{X}+D\frac{\partial^2 U}{\partial Y^2}+\frac{\partial D}{\partial Y}\frac{\partial U}{\partial Y}+\frac{\lambda\theta\sin X}{X} \quad (15)$$

$$XU\frac{\partial\theta}{\partial X}+V\frac{\partial\theta}{\partial Y}=\frac{1}{\mathrm{Pr}}\frac{\partial^2\theta}{\partial Y^2} \quad (16)$$

The corresponding boundary conditions are as follows:

$$U=V=0,\ \theta=1\ at\ Y=0 \quad (17a)$$

$$U\to\frac{\sin X}{X},\ \theta\to0\ at\ Y\to\infty \quad (17b)$$

$$D=\begin{cases}1, & |\gamma|\le\gamma_1\\ \left|\frac{\gamma}{\gamma_1}\right|^{n-1}, & \gamma_1\le|\gamma|\le\gamma_2\\ \left|\frac{\gamma_2}{\gamma_1}\right|^{n-1}, & \gamma_2\le|\gamma|\end{cases} \quad (18)$$

where, $\gamma=X\frac{\partial U}{\partial Y}$

Yao and Molla (2008) has been elaborated D in details to understand the correlation in the equation (18) (see also Bhowmick *et al.* 2013, 2014).

We observed that close to the leading edge ($X \to 0$), equation (14-16) has been solved by marching downstream that satisfying the following differential equations.

$$U + \frac{\partial V}{\partial Y} = 0 \tag{19}$$

$$V\frac{\partial U}{\partial Y} + U^2 = 1 + D\frac{\partial^2 U}{\partial Y^2} + \frac{\partial U}{\partial Y}\frac{\partial D}{\partial Y} + \lambda\theta \tag{20}$$

$$V\frac{\partial \theta}{\partial Y} = \frac{1}{\Pr}\frac{\partial^2 \theta}{\partial Y^2} \tag{21}$$

With the boundary conditions:

$$U = 0, \quad V = 0, \quad \theta = 1 \qquad \text{at} \quad Y = 0 \tag{22a}$$

$$U \to 0, \quad \theta \to 0 \quad \text{as} \quad Y \to \infty \tag{22b}$$

We have been followed the formulas of Bhowmick *et al.* (2013, 2014) to discretize the equations (14-16) and (19-21). Therefore, we can find an implicit tri-diagonal equations system, solved by double-sweep method. By using continuity equation we can solve directly the normal velocity. The solutions getting started from $X = 0$, and continuous at the downstream to $X = \pi$. Here $\Delta X = 0.0025$ and $\Delta Y = 0.005$ have been chosen for converging the results.

The skin-friction coefficient C_f and the Nusselt number Nu may be written as:

$$C_f \,\mathrm{Re}^{1/2} = X\left[D\frac{\partial U}{\partial Y}\right]_{Y=0} \tag{23}$$

$$Nu\,\mathrm{Re}^{-1/2} = -\left[\frac{\partial \theta}{\partial Y}\right]_{Y=0} \tag{24}$$

3. Results and discussion

In the study, we consider the problem of two-dimensional mixed convective boundary-layer non-Newtonian flow with an isothermal sphere of shear thinning (n = 0.6, 0.8) and of shear thickening (n = 1.2, 1.4) cases with the Newtonian fluid (n = 1.0) for the values of Pr = 0.7, 10, 50. The simulations including the distribution of viscosity, velocity and temperature; velocity gradient and the heat transfer rate in terms of the Nusselt number, $Nu\,\mathrm{Re}^{-1/2}$ for different values of n. The singularities at the leading edge has been removed by using the new power-law relation.

The simulations are quantified for the local skin-friction and Nusselt number for mixed convection parameter λ with Pr = 0.7 are entered in Table 1 for Newtonian fluid and compare with Nazar *et al.* (2002) and Salleh *et al.* (2010). The comparison shows that the results are very close and better agreement.

Tables 2-3 reveal the numerical values of local skin friction and Nusselt number for a shear-thinning (n = 0.6) fluid at various locations of X and various λ for Pr = 50. These tables show us that when the X and λ are fixed, the values of $C_f\,\mathrm{Re}^{1/2}$ decreases; on the other side $Nu\,\mathrm{Re}^{-1/2}$ are increasing. At the Table 3, we can see that for any λ the heat transfer rates are highest at the lower-stream point and then decreasing continually until the boundary-layer separates at a point.

Table 1: Comparison of the current simulations of $C_f\,\mathrm{Re}^{1/2}/X$ and $Nu\,\mathrm{Re}^{-1/2}$ for n = 0.0 while Pr = 0.7 and for different λ with Nazar *et al.* (2002) and Salleh *et al.* (2010).

λ	$C_f\,\mathrm{Re}^{1/2}/X$			$Nu\,\mathrm{Re}^{-1/2}$		
	Nazar (2002)	Salleh (2010)	Present	Nazar (2002)	Salleh (2010)	Present
-2.0	1.5581	1.5542	1.5562	0.7529	0.7519	0.7558
-1.0	2.0016	1.9973	1.9995	0.7870	0.7860	0.7901
-0.5	2.2115	2.2070	2.2093	0.8021	0.8010	0.8049
0.0	2.4151	2.4104	2.4122	0.8162	0.8150	0.8192
1.0	2.8064	2.8012	2.8038	0.8463	0.8406	0.8488
2.0	3.1804	3.1745	3.1775	0.8648	0.8636	0.8677
5.0	4.2257	4.2177	4.2217	0.9230	0.9217	0.9259
10.0	5.7995	5.7870	5.7925	0.9981	0.9967	1.0001
20.0	8.5876	8.5647	8.5724	1.1077	1.1061	1.1107

Table 2: Numerical data of the local skin friction, $C_f \,\mathrm{Re}^{1/2} / X$ for shear-thinning fluid (n = 0.6) with Pr = 50 for different λ.

x↓ λ→	-2.0	-0.5	0.0	0.5	2.0	5.0	10.0
0.0000	0.00000	0.00000	0.00000	0.00000	0.00000	0.00000	0.00000
0.5061	0.27270	0.37584	0.41471	0.45132	0.52997	0.67679	0.88254
0.9948	0.22201	0.46241	0.54035	0.61109	0.75747	1.01936	1.37426
1.5009		0.24224	0.41288	0.53729	0.76491	1.13471	1.60768
2.0071				0.20788	0.58741	1.04676	1.57785
2.4958					0.33110	0.82773	1.35511
3.0019							0.76931
3.1416							0.16165

Table 3: Numerical data of the Nusselt Number, $Nu\,\mathrm{Re}^{-1/2}$ for shear-thinning fluid (n = 0.6) with Pr = 50 for different λ.

x↓ λ→	-2.0	-0.5	0.0	0.5	2.0	5.0	10.0
0.0000	2.86707	2.99838	3.04859	3.09591	3.19709	3.38193	3.62883
0.5061	3.04499	3.37277	3.49069	3.59919	3.82448	4.21962	4.72724
0.9948	2.26847	2.88614	3.05992	3.20999	3.50177	3.97554	4.54570
1.5009		1.60113	2.03944	2.30627	2.72698	3.29735	3.90567
2.0071				0.85182	1.69181	2.36622	2.94430
2.4958					0.68939	1.37958	1.87200
3.0019							0.52512
3.1416							0.01723

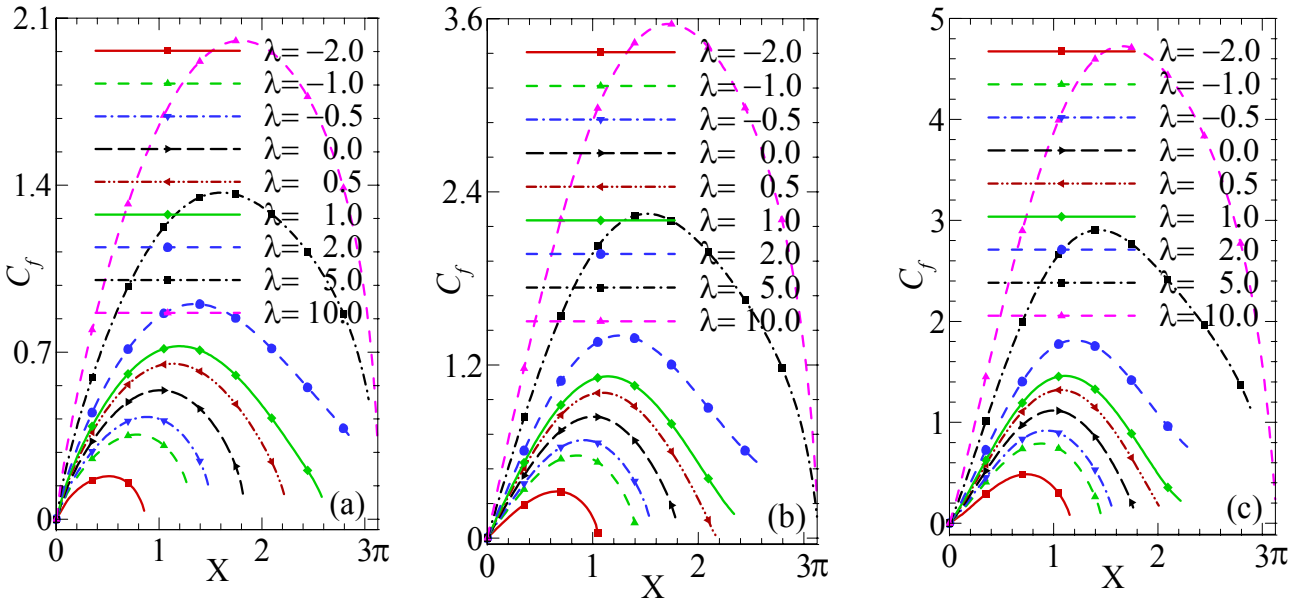

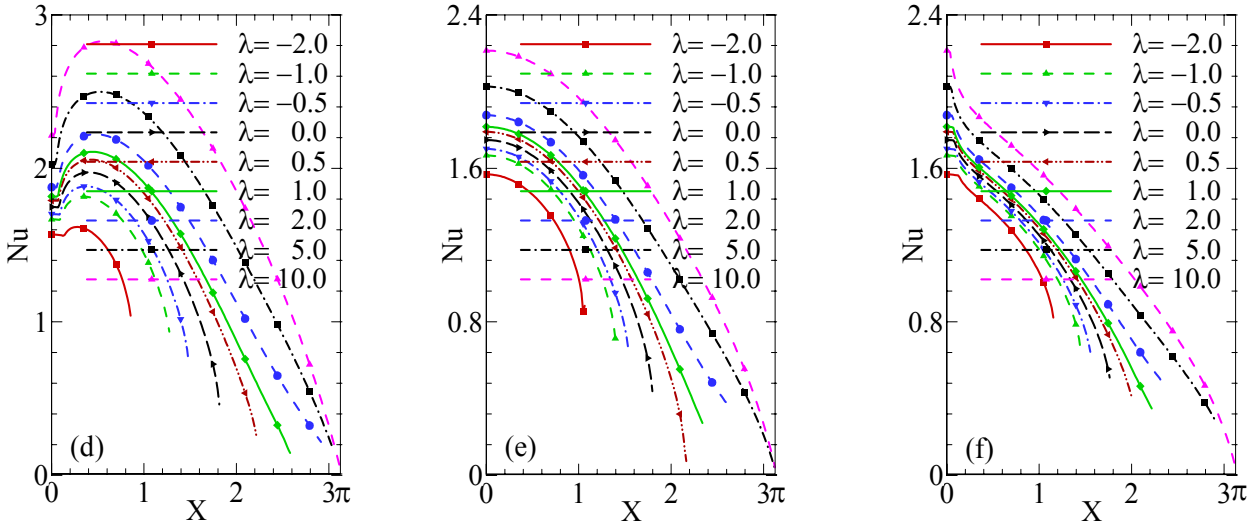

Figure 3: The variation of shear stress and heat transfer rate for power-law index n =0.6 (a, d), 1.0 (b, e) and1.4 (c, f) with different values of λ at Pr = 10.

Finally we can say that the shear stress are primarily accelerate at a particular X and then falls until the separations of boundary-layer.

The variation of shear stress and heat transfer rate have shown in Fig. 3 for various λ with Pr = 10 at the shear-thinning case (n = 0.6), the Newtonian case (n = 1.0) and shear-thickening case (n = 1.4). From these figures we observed that, for n = 0.0 the shear stresses are higher than n = 0.6 and smaller than n = 1.4; but the situation is totally opposite for heat transfer rate. Figure 3(d) reveals that the rate of heat transfer are initially increases for any λ as a particular X for shear-thinning fluid and after that decreases until the boundary-layer separates at a point. Again for the Newtonian fluid, Fig. 3(e) shows that the values of the heat transfer rate are increased at the lower edge and continually falls until the separation of boundary-layer. Moreover, Fig. 3(f) reveals that the rate of heat transfer for shear thickening fluid are decreasing slowly with respect to other two cases for any λ.

Figure 4 presents the velocity distribution at a fixed point X = 1 for n = 0.8, 1.0 and 1.2 for different λ at Pr = 10. Here, we can see that for n = 0.8 the velocity of the fluid accelerate quickly at the leading edge and increases slowly at downstream region due to the variations of the viscosity. Other hand, the velocity of the fluid for the case of n = 1.2 (shear-thickening) uniformly rises always from leading edge to down edge but the boundary-layer is relatively thinner than for the case of n = 0.8 (shear-thinning) due to more viscous of the fluid . And for n = 1.0 the velocity distribution lies between shear-thinning and shear-thickening case. We can clearly conclude that in among cases (n = 0.8, 1.0 and 1.2), the velocities of the fluid are comparatively high for large λ.

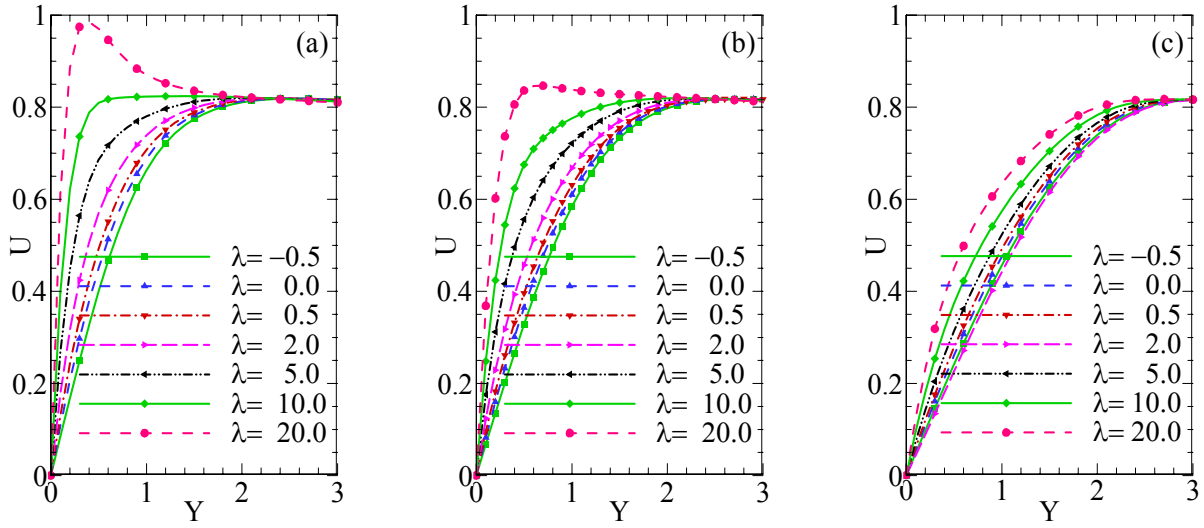

Figure 4: Velocity distributions for n = 0.8 (a), 1.0 (b) and 1.2 (c) at a fixed point X=1 for different λ at Pr = 10.

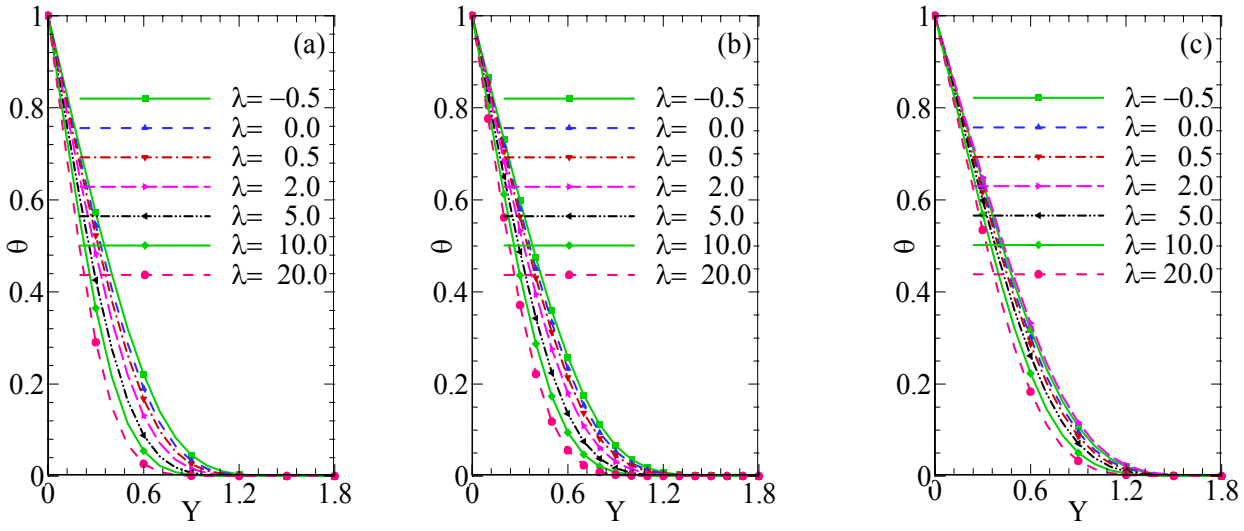

Figure 5: Temperature distributions for $n = 0.8$ (a), 1.0 (b) and 1.2 (c) at a fixed point $X = 1$ for different λ at Pr = 10.

Figure 5 reveals the temperature distribution at a fixed point $X = 1$ for $n = 0.8$, 1.0 and 1.2 for different λ at Pr = 10. Here, we can see that for $n = 0.8$ and 1.0 the variation of the fluid temperature decreases quickly at the leading edge and decreases slowly at downstream edge; therefore, the boundary-layer becomes thicken. Other hand, the temperature of the fluid for the case of $n = 1.2$ (shear-thickening) uniformly decreases from leading edge to down edge and the boundary-layer is relatively thinner than other cases due to more viscous of the fluid. We can clearly conclude that in among cases (n = 0.8, 1.0 and 1.2), the fluid temperature are comparatively small for large λ .

4. Conclusion

We have discussed the non-Newtonian mixed convective boundary-layer flow over a uniform surface temperature problem using the modified power-law method. We investigated to ordain how the flow and heat transfer features affect the mixed convective parameter, λ and the Prandtl number, Pr. Our obtained results are summarized as follows:

Regarding the Newtonian fluid (n = 1.0), for all the values of λ at Pr = 10 the heat transfer increases till obtaining the highest at the lower-stagnation point and decreases rapidly until the points of boundary-layer separations. Though, regarding the shear-thinning fluid (n = 0.6) and corresponding case of heat transfer, the values are continually increase till a particular X and then decrease until the points of boundary-layer separations. Moreover, for the shear-thickening fluid (n = 1.4) and corresponding case of heat transfer, the values are firstly decreases rapidly and then slowly decrease until the points of boundary-layer separations.

In the case of velocity distribution, for n = 0.8, the velocity increases rapidly at the initial part and increases slowly at the downstream region. Other side, for n = 1.2, the velocity at the total region consistently rises.

In the case of temperature distribution, for n = 0.8, the changing of temperature of the fluid in the boundary-layer falls quickly whenever it falls gradually at the downstream region. On the other side, regarding n = 1.2, the changing of temperature in the boundary-layer at the total region falls less rapidly.

References

Acrivos A. 1960. A Theoretical Analysis of Laminar Natural Convection Heat Transfer to Non-Newtonian Fluids, *AIChE Journal*, 6(4): 584-590.

Bhowmick S, Molla MM, Saha SC. 2013(a). Non-Newtonian Natural Convection Flow along an Isothermal Horizontal Circular Cylinder Using Modified Power-Law Model, *American Journal of Fluid Dynamics*, 3 (2): 20-30.

Bhowmick S, Molla MM, Hossain MA. 2013(b). Non-Newtonian Natural Convection Flow along a Horizontal Circular Cylinder with Uniform Surface Heat Flux, *Advances in Mechanical Engineering*, Vol. 2013, Article ID 194928.

Bhowmick S, Molla MM, Yao LS. 2014(a). Non-Newtonian Mixed Convection Flow along an Isothermal Horizontal Circular Cylinder, *Numerical Heat Transfer Part A*, 66: 509-529.

Bhowmick S, Molla MM, Yao LS. 2014(b). Non-Newtonian Mixed Convection Flow from a Horizontal Circular Cylinder with Uniform Surface Heat Flux, *Procedia Engineering* (10^{th} ICME, 2013), 90: 510-516.

Boger DV. 1977. Demonstration of upper and lower Newtonian fluid behavior in a pseudo plastic fluid, *Nature*, 265: 126-128.

Chen TS. Mocoglu A. 1977. Analysis of Mixed Forced and Free Convection about a Sphere, *Int. J. Heat Mass Transfer*, 20: 867-875.

Chen TS, Mucoglu A. 1978. Mixed Convection about a Sphere with Uniform Surface Heat Flux, *J. Heat Transfer*, 100: 542–544.

Chiang T, Ossin A, Tien CL. 1964. Laminar Free Convection from a Sphere, *ASME J. Heat Transfer*, 86: 537-542.

Huang MJ. Chen CK. 1987. Laminar Free Convection from a Sphere with Blowing and Suction, *ASME J. Heat Transfer*, 109: 529-532.

Huang MJ, Huang JS, Chou YL, Cheng CK. 1989. Effects of Prandtl Number on Free Convection Heat Transfer from a Vertical Plate to a Non-Newtonian Fluid, *Journal of Heat Transfer*, 111: 189-191.

Kim E. 1997. Natural Convection Along a Wavy Vertical Plate to Non-Newtonian Fluids, *International Journal of Heat and Mass Transfer*, 40(13): 3069-3078.

Kotouc M, Bouchet G, Dusek J. 2008. Loss of Axisymmetry in the Mixed Convection, Assisting Flow Past a Heated Sphere, *Int. J. Heat and Mass Transfer*, 51: 2686–2700.

Molla MM, and Yao LS. 2009. Mixed convection of non-Newtonian fluids along a heated vertical flat plate, *Int. J. Heat Mass Transfer*, 52: 3266-3271.

Nazar R, Amin N, Grosan T, Pop I. 2002 Free Convection Boundary Layer on an Isothermal Sphere in a Micropolar Fluid, *Int. Comm. Heat Mass Transfer*, 29(3): 377-386.

Nazar R, Amin N, Pop I. 2002. On the Mixed Convection Boundary Layer Flow about a Solid Sphere with Constant Surface Temperature, *The Arabian Journal for Science and Engineering*, 27: 117–135.

Nazar R, Amin N, Pop I. 2003. Mixed Convection Boundary Layer Flow about an Isothermal Sphere in a Micropolar Fluid, *Int. J. Thermal Sciences*, 42: 283–293.

Salleh MZ, Nazar R, Pop I. 2010. Mixed convection boundary layer flow about a solid sphere with Newtonian heating, *Arch. Mech*, 62(4): 283-303.

Yacob NAM, Nazar RM. 2006. Mixed Convection Boundary Layer on a Solid Sphere with Constant Surface Heat Flux, *Journal of Quality Measurement* and Analysis, 2: 63–74.

Yao LS, Molla MM. 2008. Non-Newtonian Fluid Flow on a Flat Plate, 1: Boundary Layer, *Journal of Thermophysics and Heat Transfer*, 22(4): 758-761.